Synthesis and ferroelectric properties of epitaxial $BiFeO_3$ thin films grown by sputtering

R. R. Das, D. M. Kim, S. H. Baek, and C. B. Eom[a)]
Department of Materials Science and Engineering, University of Wisconsin–Madison, Madison, Wisconsin 53706

F. Zavaliche, S. Y. Yang, and R. Ramesh
Department of Materials Science and Engineering, University of California, Berkeley, California 94720

Y. B. Chen and X. Q. Pan
Department of Materials Science and Engineering, The University of Michigan, Ann Arbor, Michigan 48109

X. Ke and M. S. Rzchowski
Department of Physics, University of Wisconsin–Madison, Madison, Wisconsin 53706

S. K. Streiffer
Materials Science Division, Argonne National Laboratory, Argonne, Illinois 60439

(Received 31 August 2005; accepted 19 May 2006; published online 15 June 2006)

We have grown epitaxial $BiFeO_3$ thin films with smooth surfaces on (001), (101), and (111) $SrTiO_3$ substrates using sputtering. Four-circle x-ray diffraction and cross-sectional transmission electron microscopy show that the $BiFeO_3$ thin films have rhombohedral symmetry although small monoclinic distortions have not been ruled out. Stripe ferroelectric domains oriented perpendicular to the substrate miscut direction and free of impurity phase are observed in $BiFeO_3$ on high miscut (4°) (001) $SrTiO_3$, which attributes to a relatively high value of remanent polarization ($\sim 71\ \mu C/cm^2$). Films grown on low miscut (0.8°) $SrTiO_3$ have a small amount of impure phase α-Fe_2O_3 which contributes to lower the polarization values ($\sim 63\ \mu C/cm^2$). The $BiFeO_3$ films grown on (101) and (111) $SrTiO_3$ exhibited remanent polarizations of 86 and 98 $\mu C/cm^2$, respectively. © *2006 American Institute of Physics*. [DOI: 10.1063/1.2213347]

Multiferroics belong to the family of multifunctional oxides in which ferroelectric, ferromagnetic, and ferroelastic behaviors coexist in the same materials systems. It is known that relatively few multiferroic materials exist as naturally occurring phases examples of which include $BiFeO_3$, $BiMnO_3$, $BiCrO_3$, etc.[1,2] Recently, $BiFeO_3$ multiferroics have drawn a great deal of attention due to their superior ferroelectric properties in epitaxial thin film form in comparison to counterpart bulk single crystals or ceramics.[3–7] Although the origin of enhancement of the ferroelectric and ferromagnetic responses is not clearly understood, the possibility of a high value of remanent polarization ($P_r \sim 55\ \mu C/cm^2$) and magnetization ($M_s \sim 80$ emu/cc) (Refs. 3 and 8) in (001) $BiFeO_3$ thin films (~70 nm) opens an avenue to study the host $BiFeO_3$ for various functional device applications.

Recent experimental[3,4] and theoretical[5] reports suggest that the tetragonal or monoclinic symmetry that can be induced in $BiFeO_3$ thin films by a substrate may be the cause of the high polarization (P_r) that has been observed. Most recently, Qi *et al.*[9] have claimed that (001) oriented 200 nm thick $BiFeO_3$ thin films were fully relaxed and have the bulk-like rhombohedral structure. The existence of a low symmetry monoclinic phase in (001) oriented epitaxially constrained $BiFeO_3$ thin film has also been reported by Xu *et al.*[10] Therefore, more complete structural analysis of thin films in relationship to ferroelectric and magnetic behaviors is necessary for better understanding of engineered epitaxial $BiFeO_3$ heterostructures and to clarify the properties far from bulk conditions.

Previously, it has been reported[3,11] that pulsed-laser-deposited (PLD) $BiFeO_3$ thin films on (001) $SrTiO_3$ exhibited enhanced ferroelectric response with $P_r \sim 55\ \mu C/cm^2$. There is only one report on (001), (101), and (111) oriented $BiFeO_3$ thin films in which the polarization curves of the films were projected onto the (111) easy axis,[4] and there are no reports on the growth of $BiFeO_3$ on different miscut substrates.

In this letter we report the growth and properties of high quality epitaxial $BiFeO_3$ heterostructures onto miscut (001), (101), and (111) $SrTiO_3$ substrates using high-rate off-axis sputtering.[12] Sputtering allows us to grow complex oxide thin films with extremely smooth surfaces.[13] The thicknesses of the films were varied from 60 to 600 nm to understand crystal structure, strain relaxations, and its influence on the ferroelectric and magnetic properties. The influence of miscut on the microstructure, ferroelectric domain structure, and ferroelectric properties of the films on (001) $SrTiO_3$ substrates was also investigated. Miscut angles of 0.8° and 4° toward [100] were explored. For electrical characterization, films that were deposited on epitaxial $SrRuO_3$ bottom electrodes of thickness 100 nm were grown on the $SrTiO_3$ substrates using 90° off-axis sputtering.[14] $BiFeO_3$ thin films were grown at a substrate temperature of 690 °C from the targets with 5% excess Bi_2O_3 in order to compensate for Bi volatilization from the films.

Figure 1(a) shows a scanning probe micrograph of a $BiFeO_3$ film grown on 4° miscut (001) $SrTiO_3$. As expected, the steps and terraces align perpendicular to the miscut direction [the arrow in Fig. 1(b) points along the miscut direc-

[a)]Author to whom correspondence should be addressed; electronic mail: eom@engr.wisc.edu

 © 2006 American Institute of Physics

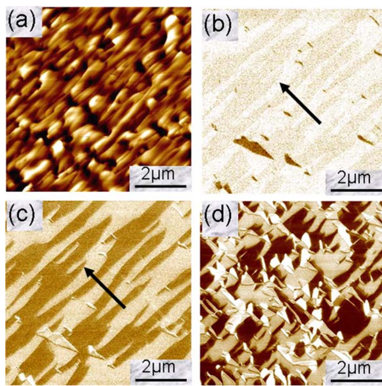

FIG. 1. (Color online) (a) AFM topography of $BiFeO_3$ films grown on 4° miscut (001) $SrTiO_3$. (b) Out-of-plane and (c) in-plane PFM images of the 600 nm thick $BiFeO_3$ film grown on 4° miscut (001) $SrTiO_3$. The arrow in (b) shows the substrate miscut direction. The scan size is $7\times 7\ \mu m^2$, and the PFM images were recorded at an ac bias of $3V_{pp}$ and 6.39 kHz. (d) In-plane PFM image of 600 nm $BiFeO_3$ film on 0.8° miscut (001) $SrTiO_3$ that shows four variants of domain patterns.

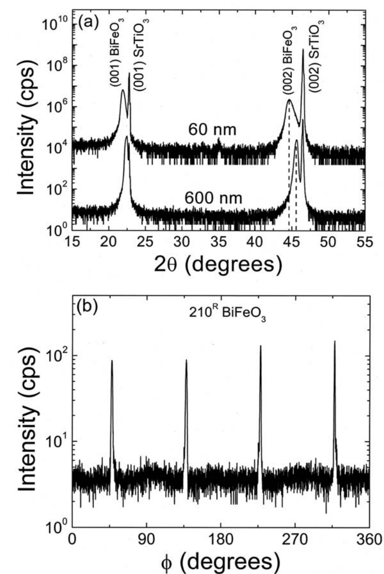

FIG. 2. (a) X-ray diffraction θ-2θ scans for 60 and 600 nm $BiFeO_3$ thin films on (001) $SrTiO_3$. (b) Off-axis azimuthal ϕ scan of 210^R rhombohedral $BiFeO_3$ reflections.

tion]. A root-mean-square (rms) surface roughness is approximately 30 Å, which is much smoother than previously reported PLD grown films.[3,4] Images and a line trace along the miscut direction show evidence of multiple unit cell high bunched steps. We have also observed similar kind of step bunching of $SrRuO_3$ films on high miscut $SrTiO_3$ substrates.[15]

It was observed that the miscut angle of the substrates has a strong influence on the microstructure of the films.[16] It appears that the volatile species, Bi, is incorporated and retained more effectively for shorter terrace length and a higher density of steps and kinks. Thus, we believe that important roles of substrate miscut include more robust maintenances of film stoichiometry by decreasing the propensity for volatile species to desorb and to maintain the step-flow growth up to large thicknesses. We have also observed similar behavior for $Pb(Zr,Ti)O_3$ and $0.67Pb(Mg_{1/3}Nb_{2/3})$ $-0.33PbTiO_3$ (PMN-PT) films deposited on miscut (001) $SrTiO_3$ substrates.[17]

Out-of-plane and in-plane piezoforce microscopy (PFM) images shown in Figs. 1(b) and 1(c) were recorded simultaneously with the topographic scan shown in Fig. 1(a). The predominantly white tone in the out-of-plane PFM image shown in Fig. 1(b) indicates that the ferroelectric polarization points mainly downwards in the as-grown film, while the in-plane PFM image in Fig. 1(c) reveals the presence of stripe domains. These domains run perpendicular to the miscut direction and exhibit a completely different pattern than observed for $BiFeO_3$ films grown under the same conditions on low miscut (0.8°) (001) $SrTiO_3$ substrates, as shown in Fig. 1(d).[18] It clearly shows four variants of domain patterns.

The crystal structure, epitaxial orientation, crystalline quality, and three-dimensional strain states of the $BiFeO_3$ thin films were determined using a four-circle x-ray diffractometer with a high resolution four-bounce monochromator. $BiFeO_3$ in the bulk form is reported to have a highly distorted rhombohedral crystal structure[19] ($a_0{}^R=5.6343$ Å, $\alpha^R=59.348°$) but can be indexed based on pseudocubic[4] lattice ($a_0=3.96$ Å). (Note that superscript R stands for the rhombohedral structure; otherwise we use pseudocubic indices.) Figure 2(a) shows the x-ray θ-2θ scans of 60 and 600 nm thick $BiFeO_3$ on (001) $SrTiO_3$. There is a systematic variation of the $00l$ peaks towards lower diffraction angle with reduced thickness. This indicates that the out-of-plane lattice parameters of thinner films are larger than thicker. The full width at half maximum (FWHM) of the rocking curve for the 002 $BiFeO_3$ reflection for 60–600 nm thick films ranges from 0.35° to 0.42°, which is relatively narrow and confirmed the high crystalline quality of the films.

The in-plane epitaxial arrangement of the (001) $BiFeO_3$ films was studied using azimuthal ϕ scans. The substrate orientation was established via ϕ scans of 101 reflections of the (001) $SrTiO_3$ which were defined to be at $\phi=0°$, 90°, 180°, and 270°. The pseudocubic lattice 101^C reflections of $BiFeO_3$ were found to be shifted ±0.5° from these values for cubic or c-axis tetragonal structure. Also multiple peaks of $BiFeO_3$ were observed from off-axis ϕ scans. This suggests that $BiFeO_3$ does not have tetragonal symmetry. To determine the crystal symmetry of the films, we have measured ϕ scans for the rhombohedral nondegenerate 210^R reflection of $BiFeO_3$, as shown in Fig. 2(b). Even thinner films of 60 nm show the same behavior. This confirms the rhombohedral structure of the films, the possibility of small monoclinic distortions from the rhombohedral structure has not been ruled out. Our structural data confirm the rhombohedral structure of the films even at a thickness of 60 nm.

The P-E hysteresis loops were measured using a Radiant Technology RT6000 ferroelectric tester, with an external frequency generator, at frequencies of 16–20 kHz. Pt top electrodes with diameters of 25, 50, 100, and 200 μm were lithographically patterned using a lift-off process in order to measure the electrical properties of the films. Hysteresis loops of 200 nm thick films grown on miscut (001) $SrTiO_3$ are shown in Fig. 3(a). The remanent polarizations ($P_r\sim\Delta P/2$) were 63±5 and 71±5 $\mu C/cm^2$ for the films grown on 0.8° and 4° miscut (001) $SrTiO_3$ substrates, respectively. However, the miscut angle dependence of polarization is less conspicuous for 600 nm thick films.

We have also grown 600 nm thick films on (101) and (111) oriented $SrTiO_3$, and the corresponding polarization data are shown in Fig. 3(b), along with the data for (001) films. Remanent polarization values of 86±5 and 98±5 $\mu C/cm^2$, which are approximately $\sqrt{2}$ and $\sqrt{3}$ times

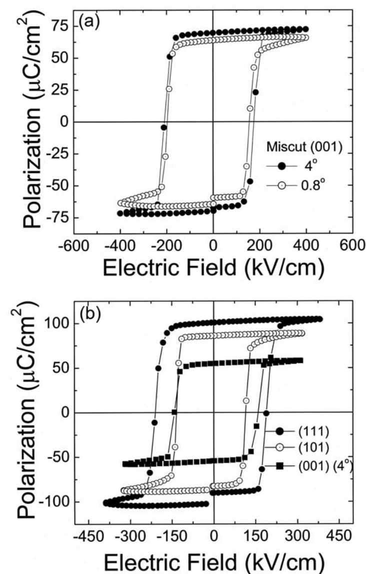

FIG. 3. (a) *P-E* hysteresis loops of 200 nm $BiFeO_3$ films on 0.8° and 4° miscut (001) $SrTiO_3$. (b) Hysteresis loops of 600 nm thick (001), (101), and (111) oriented $BiFeO_3$ films. The hysteresis loops were measured on capacitors with top electrode diameter of 200 μm.

the P_r value for (001) $BiFeO_3$ films, were measured for the (101) and (111) films, respectively. The observed remanent polarization values are relatively higher than the ones previously reported for PLD grown (001) $BiFeO_3$ films.[3,4,11]

The microstructures of $BiFeO_3$ thin films were characterized by cross-sectional transmission electron microscopy (TEM). Figures 4(a) and 4(b) are cross-sectional bright field images taken using the 011 reflection of the 200 nm $BiFeO_3$ thin films on (001) $SrTiO_3$ substrates with 4° and 0.8° miscuts, respectively. Both selected area electron diffraction pattern [as shown as an inset in Figs. 4(a) and 4(b)] and high resolution lattice images reveal the rhombohedral lattice distortion of the $BiFeO_3$ films. However, the microstructures of these two $BiFeO_3$ thin films are different. As shown in Fig. 4(a), there are parallel fringes running along the {011} direction and perpendicular to the miscut direction. They are 71° ferroelectric domains, confirmed by both high resolution lattice images and selected area electron diffraction. The average spacing of the 71° domain walls is about 250 nm. In contrast, there are a small amount of α-Fe_2O_3 (space group $R3C$) phase [indicated by black arrows in Fig. 4(b)] embedded in $BiFeO_3$ matrix. A selected area electron diffraction pattern from a region consisting of both an impurity phase particle and the $BiFeO_3$ film is shown as an inset in Fig. 4(b). The crystallographic orientation relationship between $BiFeO_3$ and α-Fe_2O_3 was determined to be [421] (112) $BiFeO_3$‖[112] (132) α-Fe_2O_3. In addition, we have also observed boundaries formed by four-variant domains and/or stacking faults. This is consistent with the result that the $BiFeO_3$ films grown on 4° miscut $SrTiO_3$ show higher spontaneous polarization than the film grown on 0.8° miscut $SrTiO_3$.

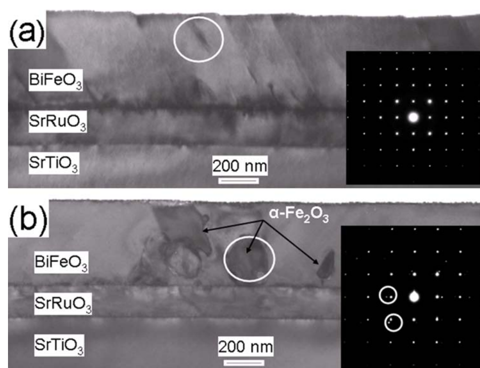

FIG. 4. (Color online) Low magnification cross-sectional TEM micrographs of $BiFeO_3$ thin film on (a) 4° miscut (001) $SrTiO_3$ and (b) 0.8° miscut (001) $SrTiO_3$ substrates. Inset shows the diffraction patterns of the respective $BiFeO_3$ matrix and α-Fe_2O_3 for the white circle region. The diffraction spots coming from α-Fe_2O_3 are indicated by white arrows.

In summary, we have grown high quality epitaxial $BiFeO_3$ thin films using magnetron sputtering. We observed that the films grown on high miscut (4°) (001) $SrTiO_3$ substrates have stripe ferroelectric domains and show enhanced value of remanent polarization ($\sim$71 $\mu C/cm^2$). The films on low miscut (0.8°) $SrTiO_3$ have significant amount of four-variant ferroelastic boundaries and second phases of α-Fe_2O_3 which acts as pinning centers for 180° domain switching and resulted into lower value remanent polarization.

This work was supported by the National Science Foundation under Grant Nos. DMR-0313764, DMR-0315633 (for HRTEM), and ECS-0210449, ONR under Grant No. N000140510559, and a David & Lucile Packard Fellowship to one of the authors (C.B.E.). The authors wish to acknowledge the support by the University of Maryland NSF-MRSEC under Grant No. DMR 00-80008. Work at Argonne National Laboratory was supported by the U.S. Department of Energy, Office of Science, Office of Basic Energy Sciences, under Contract No. W-31-109-Eng-38.

[1]G. A. Smolenskii and I. E. Chupis, Usp. Fiz. Nauk **137**, 415 (1982); Sov. Phys. Usp. **25**, 475 (1982).
[2]N. A. Hill, J. Phys. Chem. B **104**, 6694 (2000).
[3]J. Wang, J. B. Neaton, H. Zheng, V. Nagarajan, S. B. Ogale, B. Liu, D. Viehland, V. Vaithyanathan, D. G. Schlom, U. V. Waghmare, N. A. Spaldin, K. M. Rabe, M. Wuttig, and R. Ramesh, Science **299**, 1719 (2003).
[4]J. Li, J. Wang, M. Wuttig, R. Ramesh, N. Wang, B. Ruette, A. P. Pyatakov, A. K. Zvezdin, and D. Viehland, Appl. Phys. Lett. **84**, 5261 (2004).
[5]C. Ederer and N. A. Spaldin, Phys. Rev. B **71**, 224103 (2005).
[6]J. R. Teague, R. Gerson, and W. J. James, Solid State Commun. **8**, 1073 (1970).
[7]Y. P. Wang, L. Zhou, M. F. Zhang, X. Y. Chen, J. M. Liu, and Z. G. Liu, Appl. Phys. Lett. **84**, 1731 (2004).
[8]J. Wang, A. Scholl, H. Zheng, S. B. Ogale, D. Viehland, D. G. Schlom, N. A. Spaldin, K. M. Rabe, M. Wuttig, L. Mohaddes, J. Neaton, U. V. Waghmare, T. Zhao, and R. Ramesh, Science **307**, 1203b (2005).
[9]X. Qi, M. Wei, Y. Lin, Q. Jia, D. Zhi, J. Dho, M. G. Blamire, and J. L. M. Manus-Driscoll, Appl. Phys. Lett. **86**, 071913 (2005).
[10]G. Xu, H. Hiraka, G. Shirane, J. Li, J. Wang, and D. Viehland, Appl. Phys. Lett. **86**, 182905 (2005).
[11]K. Y. Yun, M. Noda, M. Okuyama, H. Saeki, H. Tabata, and K. Saito, J. Appl. Phys. **96**, 3399 (2004).
[12]D. M. Kim, R. R. Das, S. H. Baek, and C. B. Eom (unpublished).
[13]C. B. Eom, A. F. Marshall, S. S. Laderman, R. D. Jacowitz, and T. H. Geballe, Science **249**, 1549 (1990).
[14]C. B. Eom, R. J. Cava, R. M. Fleming, J. M. Phillips, R. B. Vandover, J. H. Marshall, J. W. P. Hsu, J. J. Krajewski, and W. F. Peck, Science **258**, 1766 (1992).
[15]R. A. Rao, Q. Gan, and C. B. Eom, Appl. Phys. Lett. **71**, 1171 (1997).
[16]S. D. Bu, M. K. Lee, C. B. Eom, W. Tian, X. Q. Pan, S. K. Streiffer, and J. J. Krajewski, Appl. Phys. Lett. **79**, 3482 (2001).
[17]D. M. Kim, S. H. Baek, R. R. Das, and C. B. Eom (unpublished).
[18]F. Zavaliche, S. Y. Yang, P. Shafer, R. Ramesh, R. R. Das, D. M. Kim, and C. B. Eom, Appl. Phys. Lett. **87**, 182912 (2005).
[19]F. Kubel and H. Schmid, Acta Crystallogr., Sect. B: Struct. Sci. **B46**, 698 (1990).